

1
2
3
4
5
6
7
8
9
10
11
12
13
14
15
16
17
18
19
20
21
22
23
24
25
26
27
28
29
30
31
32

Supplementary Information for

**Efficient advanced reduction with cobalt phthalocyanine-
decorated N-doped mesoporous carbon**

Mengjiao Xu, Kaizhi Wang, Wendi Guo, Zehui Sun, Mugeng Chen, Yongmei Liu*,
Yong Cao*

*Shanghai Key Laboratory of Molecular Catalysis and Innovative Materials, State Key
Laboratory of Porous Materials for Separation and Conversion, Department of
Chemistry, Fudan University, Shanghai 200433, China*

**Corresponding author*

E-mail: ymliu@fudan.edu.cn (Yongmei Liu), yongcao@fudan.edu.cn (Yong Cao)

33 1. Experimental section

34 1.1 Materials

35 Pyrrole (99%), piperidine (99%) and formic acid (99%) were purchased from
36 Alfa-Aesar. Ammonium persulfate ($(\text{NH}_4)_2\text{S}_2\text{O}_8$, 98%), Cobalt phthalocyanine (CoPc,
37 99%), $\text{K}_2\text{Cr}_2\text{O}_7$ (99%) and 2-methylimidazole (2-MeIm, 98%), sodium chloride (NaCl,
38 99.5%), sodium sulfate (Na_2SO_4 , 99%), potassium chloride (KCl, 99.5%), ammonium
39 chloride (NH_4Cl , 99.5%), sodium nitrate (NaNO_3 , 99%) were obtained from Aladdin
40 Industrial Inc. Colloidal silica (Ludox-HS-40, 40 wt% suspension in H_2O), NaOH
41 (99%), ethanol (EtOH, 99.7%), N,N-dimethylformamide (DMF, 99.5%), silver nitrate
42 (AgNO_3 , 99.8%), cobalt nitrate hexahydrate ($\text{Co}(\text{NO}_3)_2 \cdot 6\text{H}_2\text{O}$, 98.5%), zinc nitrate
43 hexahydrate ($\text{Zn}(\text{NO}_3)_2 \cdot 6\text{H}_2\text{O}$, 99.0%), methanol (MeOH, 99.7%), phosphoric acid
44 (H_3PO_4 , 85%), potassium carbonate (K_2CO_3 , 99.5%), and propylene carbonate (98%)
45 were purchased from Sinopharm Chemical Reagent Co., Ltd. 5,5-dimethyl-1-pyrroline
46 N-oxide (DMPO, 97%) was obtained from the Macklin Biochemical Co. Ltd
47 (Shanghai, China). All the reagents were used as received without further purification.

48 1.2 Characterization

49 The crystal structure of all catalysts was characterized by Bruker D8 Advance X-
50 ray diffractometer using the Ni-filtered $\text{Cu K}\alpha$ radiation source at 40 kV and 40 mA.
51 Transmission electron microscopy (TEM) images were taken by a JEOL JEM 2011
52 electron microscope operating at 200 kV. High-angle annular dark-field scanning
53 transmission electron microscopy (HAADF-STEM) images were obtained on a JEM-
54 2100F electron microscope with a HAADF detector operating at 200 kV. The loading
55 amounts of Co in the samples and the amount of Co species in Cr(VI) solution were
56 determined by inductively coupled plasma optical emission spectroscopy (ICP-OES)
57 using PerkinElmer Optima 2100DV spectrometer. The BET specific surface areas of
58 the catalysts were determined by adsorption desorption of N_2 at $-196\text{ }^\circ\text{C}$, using
59 Micromeritics Tristar 3000 equipment. Sample degassing was carried out at $300\text{ }^\circ\text{C}$
60 prior to acquiring the adsorption isotherm. The X-ray photoelectron spectroscopy

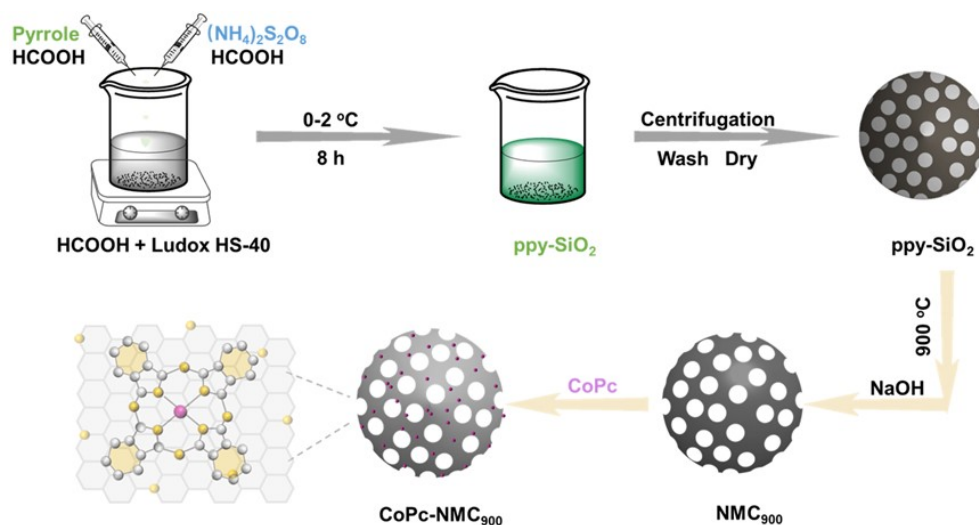
61 (XPS) measurements were performed with a Perkin Elmer PHI 5000C
62 spectrophotometer with Mg K α radiation (1253.6 eV). The binding energy (BE) scale
63 was calibrated by referencing the C 1s peak of adventitious carbon to 284.6 eV. The
64 relationship between zeta potential and pH was studied through a Zeta sizer Nano
65 instrument (ZS90, Malvern, U.K.), which was performed by adjusting the pH of the
66 samples with variable amounts of FA and 0.1 M NaOH solutions. EPR using DMPO
67 as the spin-trapping agent for the hydrogen radicals analysis was conducted with a
68 Bruker A300 spectrometer. The electrochemical impedance spectroscopy (EIS) was
69 conducted on a CHI-660E electrochemical workstation. Extended X-ray absorption fine
70 structure (EXAFS) measurements at Co K-edge under fluorescence mode were
71 performed at the BL14W1 in Shanghai Synchrotron Radiation Facility (SSRF) using a
72 Lytle detector. The electron beam energy was 3.5 GeV and the stored current was 230
73 mA (top-up). A 38-pole wiggler with the maximum magnetic field of 1.2 T inserted in
74 the straight section of the storage ring was used. The station was operated with a fixed-
75 exit double-crystal Si (111) monochromator. Co foil were used as standard reference
76 materials and the X-ray absorption data were recorded in transmission mode using ion
77 chambers. The raw data analysis was performed using IFEFFIT software package
78 according to the standard data analysis procedures.¹ The spectra were calibrated,
79 averaged, pre-edge background subtracted, and post-edge normalized using Athena
80 program in IFEFFIT software package. The Fourier transformation of the k³-weighted
81 EXAFS oscillations, $k^3 \cdot \chi(k)$, from k space to R space was performed to obtain a radial
82 distribution function. And data fitting was done by Artemis program in IFEFFIT.¹

83 **1.3 Synthesis of polypyrrole-derived mesoporous carbons**

84 The specific synthesis procedures are shown in **Scheme S1**. Mesoporous carbons
85 was achieved according to the method developed by Asefa.² Firstly, FA solution (300
86 mL, 1M) is fully cooled to 0~2 °C. Then, 60 mmol pyrrole (5.59 g) is dissolved in 90
87 mL of FA solution (1 mol·L⁻¹) to obtain solution A. Dissolving 60 mmol (NH₄)₂S₂O₈
88 (13.70 g) in 90 mL of the FA solution to obtain solution B. Ludox HS-40 silica beads
89 solution (40 wt% aqueous solution, 48 g) is added dropwise to the remaining 180 mL

90 of solution, and dispersed by stirring for a few minutes to obtain solution C. Two
 91 syringe pumps to inject solution A and solution B into solution C under stirring
 92 condition at the same time. During the injection, use an ice-water bath to keep the
 93 solution temperature at 0 °C for 8 h. The resulting dark green solid was separated by
 94 decantation and washed with water and ethanol. Dry it overnight in vacuum to obtain
 95 dark green solid PPy-SiO₂. PPy-SiO₂ is ground, sieved, and pyrolyzed at high
 96 temperature under Ar atmosphere. The specific heating conditions are heating from 25
 97 °C to 300 °C at a rate of 1 °C·min⁻¹ for 3 h, then increasing to 600-900 °C at a rate of
 98 10 °C·min⁻¹ for 2 h, and then naturally cool to 25 °C. A black powder of NMC_T-SiO₂
 99 was obtained. The obtained NMC_T-SiO₂ is etched with 1 mol·L⁻¹ NaOH solution at 100
 100 °C for 48 h to dissolve the SiO₂. Then, it was washed with water to neutrality and dried
 101 under vacuum to obtain the final NMC_T carrier.

102 **Scheme S1** The specific synthesis process for CoPc-NMC₉₀₀.



103 1.4 Synthesis of CoPc-NMC₉₀₀ materials

104 CoPc-NMC₉₀₀ were prepared by an impregnation method. Briefly, 200 mg support
 105 was dispersed in 20 mL DMF containing suitable amount of CoPc, and thereby being
 106 stirred at 25 °C overnight. After removing the solvent by rotary evaporation, the
 107 resultant product was vacuum-dried at 125 °C for 12 h.

108 1.5 Synthesis of Co-CN_{ZIF}

109 The all inorganic Co-CN_{ZIF} were synthesized via pyrolysis of Co-doped ZIF-8
110 (Zeolitic Imidazolate Frameworks-8).¹ A solution of 2-MeIm (13.4 g, 163.2 mmol) in
111 408 mL MeOH was added into a mixed solution of Co(NO₃)₂·6H₂O (0.116 g, 0.4 mmol)
112 and Zn(NO₃)₂·6H₂O (5.95 g, 20 mmol) in 408 mL MeOH. After stirred at 25 °C for 24
113 h, the obtained precipitates were collected and washed with MeOH and then vacuum
114 dried at 25 °C overnight. Subsequently, as-prepared precursor was heated at 900 °C for
115 4 h under flowing Ar (100 mL·min⁻¹) followed by cooling down to 25 °C naturally.

116 **1.6 Catalytic reduction of Cr(VI) to Cr(III)**

117 Typically, 50 mg catalyst and 4.3 mmol FA solution were added in 50.0 mL
118 K₂Cr₂O₇ solution (50 ppm for Cr(VI)) at 25 °C with a pH of ca. 3.5. All reactions were
119 monitored through UV-vis spectrophotometer (Shimadzu UV-1800) by observing
120 variations in the absorption intensity of Cr(VI) at 350 nm wavelength. Controlling
121 experiments were carried out using the same dosage of the different catalysts in the
122 presence or absence of FA. The influences of co-existing inorganic anions, initial
123 Cr(VI) or FA concentration, solution pH, and temperature on the efficiency of the
124 Cr(VI) reduction were carried out. The catalytic durability was performed at least five
125 times for any given conditions, in which catalysts were recycled by centrifugation,
126 washing with water and drying overnight after each cycle.

127 **1.7 Controlling experiments**

128 H₃PO₄ and piperidine were used as selective poisoners for Py-N and Co-N₄ sites,
129 respectively. H₃PO₄ was pre-adsorbed on catalyst while piperidine was added to
130 reaction system directly.³⁻⁴ To prepare H₃PO₄-pre-adsorbed sample, 60 mg 0.4% CoPc-
131 NMC₉₀₀ was soaked in 5 mol·L⁻¹ H₃PO₄ solution (6 mL) for 1 h at 25 °C under stirring.
132 The sample was collected by centrifugation, wash with water to neutral and then dried
133 at 80 °C overnight to obtain H₃PO₄-pre-adsorbed 0.4% CoPc-NMC₉₀₀ sample. The
134 sample was then evaluated in Cr(VI) reduction reaction under ambient air condition as
135 described above. In order to eliminate the pre-adsorbed H₃PO₄, the recovered CoPc-
136 NMC₉₀₀ catalyst with pre-adsorbed H₃PO₄ was rinsed with a 1 mol/L K₂CO₃ solution

137 (10 mL) at room temperature for 15 minutes. Following centrifugation, it was washed
138 with water and then dried at 110 °C overnight. For piperidine spiking experiment,
139 piperidine (146 mg, 1.5 mmol), water (145 μL, 8 mmol) was added into the $K_2Cr_2O_7$
140 solution, then FA was dropped in the solution.

141

142

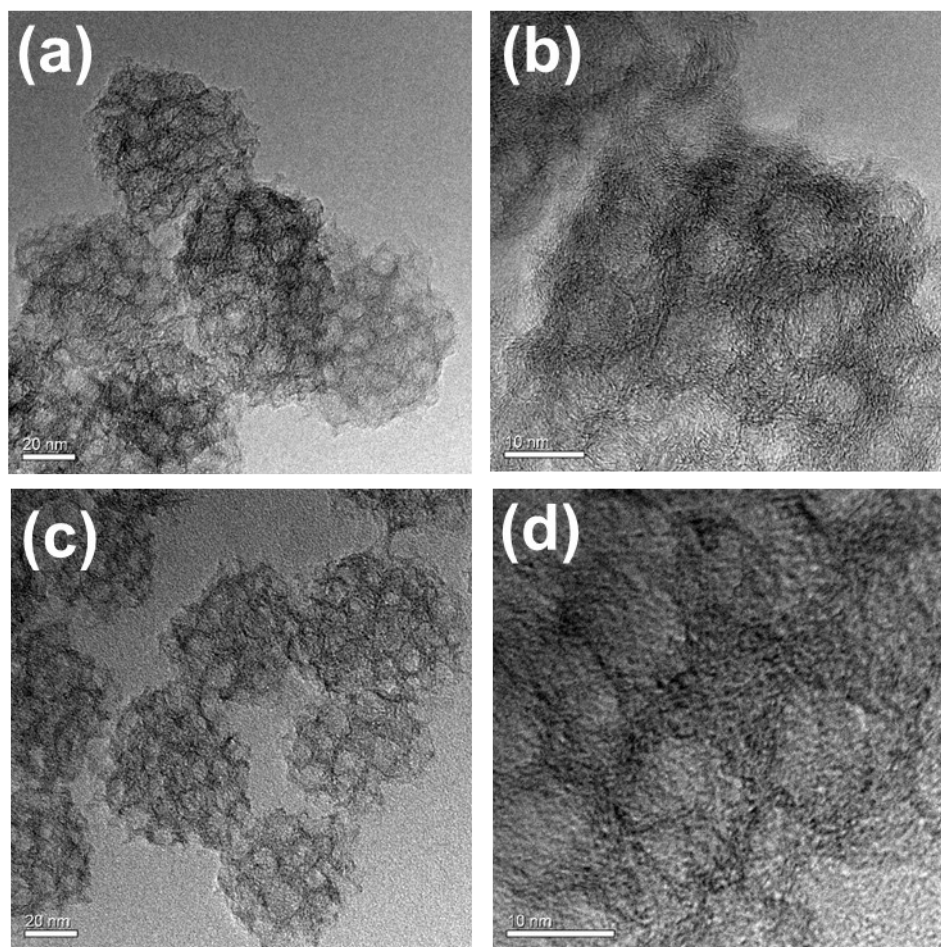
143

144

145

146

147 **2. Supplementary data (Fig. S1-17/Table S1-7)**



148

149

Fig. S1 TEM images of (a-b) NMC₉₀₀, (c-d) 0.4% CoPc-NMC₉₀₀.

150

151 Table S1 The BET Surface Area and Pore Diameter for the as-prepared samples.

Entry	Catalysts	S _{BET} (m ² ·g ⁻¹)	Pore volume(cm ³ /g)	Pore size (nm)
1	NMC ₉₀₀	564	1.566	11.1
2	0.2% CoPc-NMC ₉₀₀	520	1.466	11.1
3	0.4% CoPc-NMC ₉₀₀	408	1.403	10.7
4	1% CoPc-NMC ₉₀₀	397	1.310	10.2
5	0.4% CoPc-NMC ₉₀₀ (after 5 cycles)	401	1.399	10.5

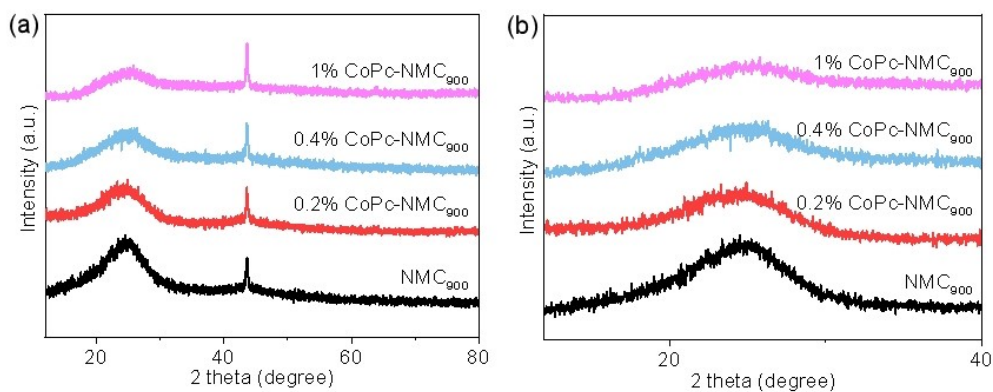
152

153

154 Table S2 The contents of Co element loading (wt%) for various samples by EDS
 155 analysis and the turnover frequency (TOF).
 156

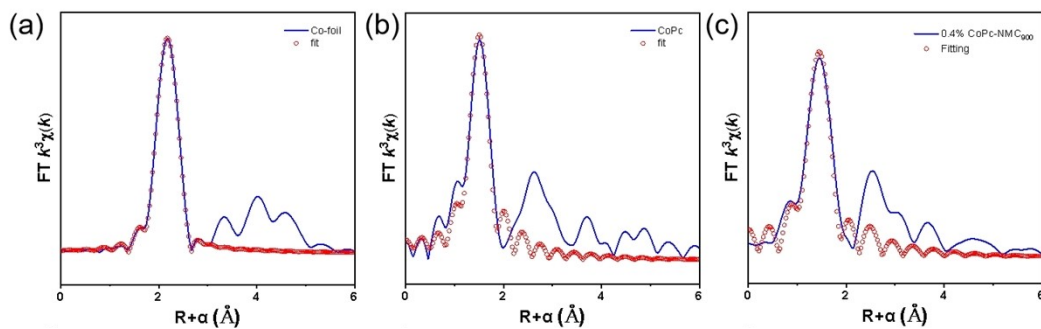
Entry	Catalysts	Loading (wt%)	TOF ($\mu\text{mol}\cdot\text{s}^{-1}\cdot\text{g}^{-1}$)
1	0.2% CoPc-NMC ₉₀₀	0.21	14.2
2	0.4% CoPc-NMC ₉₀₀	0.39	18.1
3	0.4% CoPc-NMC ₉₀₀ (after 5 cycles)	0.38	17.9
4	1% CoPc-NMC ₉₀₀	0.98	15.4
5	0.4% CoPc-TiO ₂	0.41	2.6
6	0.4% CoPc-C	0.39	3.1
7	1% Co-CN _{ZIF}	0.89	14.2

157
 158
 159
 160
 161
 162



163
 164
 165
 166

Fig. S2 XRD pattern of the various samples.



167

168 Fig. S3 EXAFS fitting of (a) Co foil, (b) CoPc and (c) 0.4% CoPc-NMC₉₀₀ in R-space.

169

170 Table S3 EXAFS fitting parameters at the Co K-edge for various samples ($S_0^2=0.73$) .

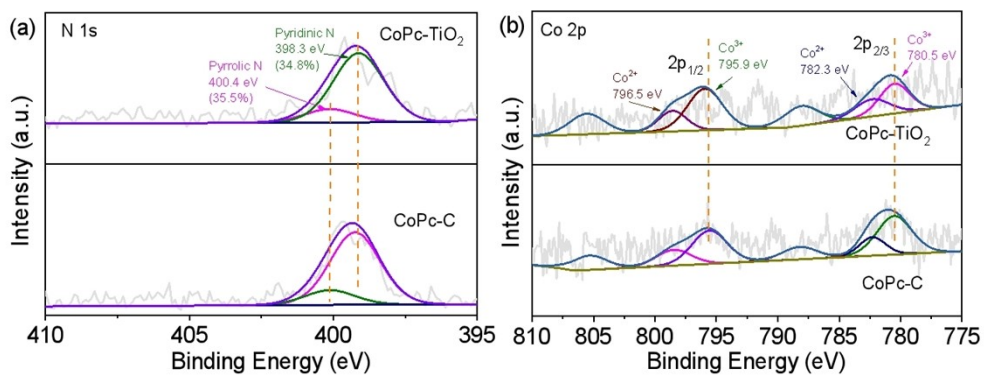
Entry	Catalysts	Shell	CN ^a	R ^b (Å)	σ^{2c} (Å ²)	ΔE_0^d (eV)	R factor
1	Co-foil	Co-Co	12	2.49±0.01	0.0063	7.2±0.3	0.0010
2	CoPc	Co-N	4	1.91±0.01	0.0023	6.4±2.4	0.0117
3	0.4% CoPc-NMC ₉₀₀	Co-N	4.2±0.4	1.90±0.01	0.0027	3.3±2.4	0.0118

171 ^a CN: coordination numbers; ^b R: bond distance; ^c σ^2 : Debye-Waller factors; ^d ΔE_0 : the inner potential

172 correction. R factor: goodness of fit.

173

174



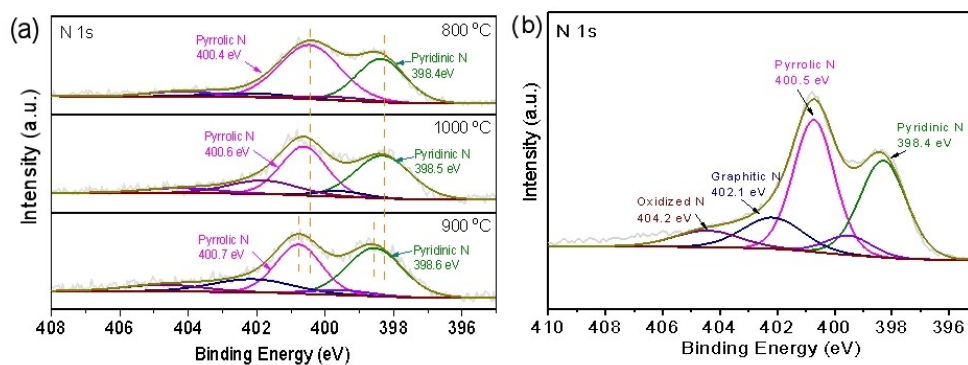
175

176

Fig. S4 XPS of (a) N 1s and (b) Co 2p for CoPc-TiO₂ and CoPc-C.

177

178



179
 180 Fig. S5 XPS spectra of (a) N 1s of CoPc-NMC calcined at different temperature and
 181 (b) N 1s of CoPc & NMC₉₀₀.

182

183

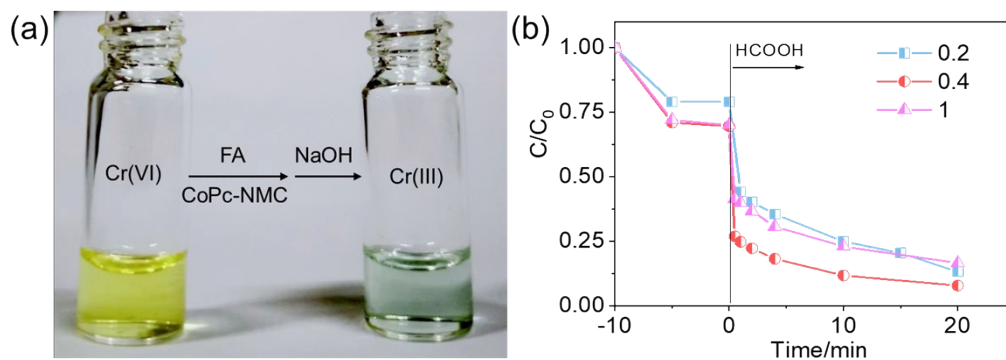
184

185 Table S4. Comparison of various catalysts with the present work for the reduction of
 186 Cr(VI) .

Entry	Catalysts	FA/Cr	TOF ($\mu\text{mol}\cdot\text{s}^{-1}\cdot\text{g}^{-1}$)	Reference
1	Ni@NC-700	1076	3.2	[1]
2	Ni-N-C600	260	9.2	[2]
3	Ni@NMC550	520	2.0	[3]
4	Ni@N-CNTs/N-G	1062	6.3	[4]
5	Ni@carbon450	313	5.4	[5]
6	Co-RGO	36	2.8	[6]
7	0.4% CoPc-NMC ₉₀₀	90	18.1	Our work

187

188



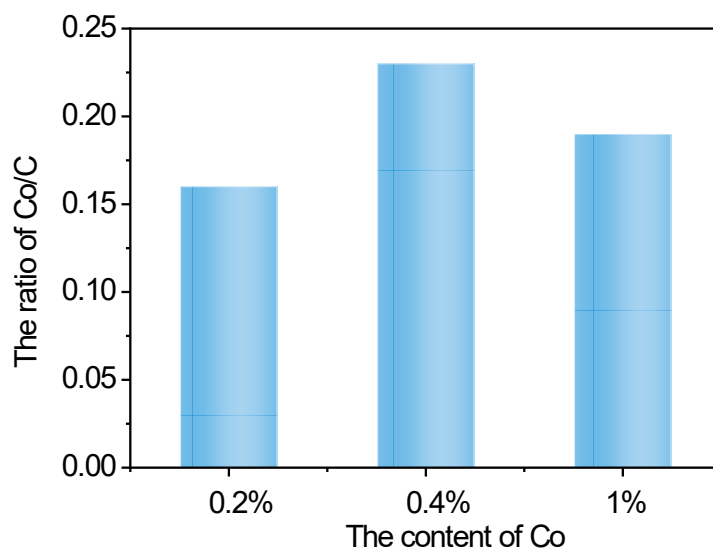
189

190 Fig. S6 (a) The color change of the Cr(VI) solution after reaction by adding NaOH. (b)

191 The influence of CoPc content (wt%) on the catalytic reduction. (Reaction conditions:

192 50 mL Cr(VI) (50 ppm), 4.3 mmol FA, 50 mg catalyst, 25 °C.)

193



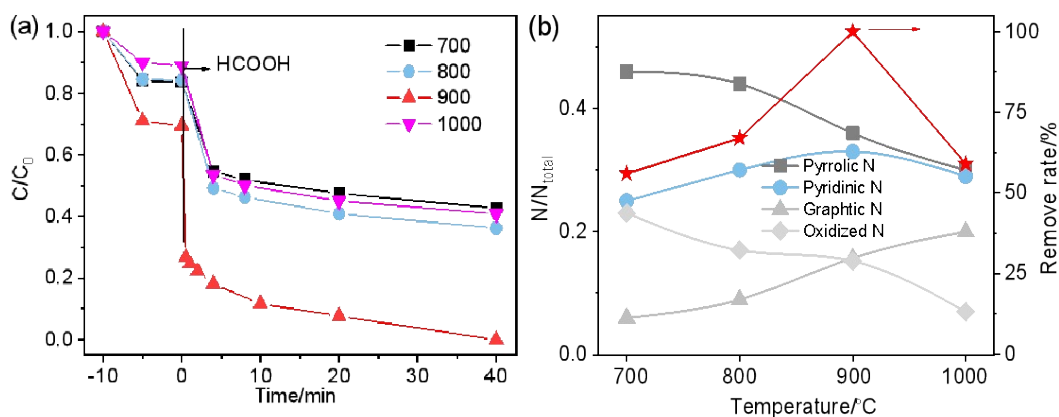
194 Fig. S7 Relationship between the content of Co and the XPS-determined surface Co/C

195 ratio.

196

197

198



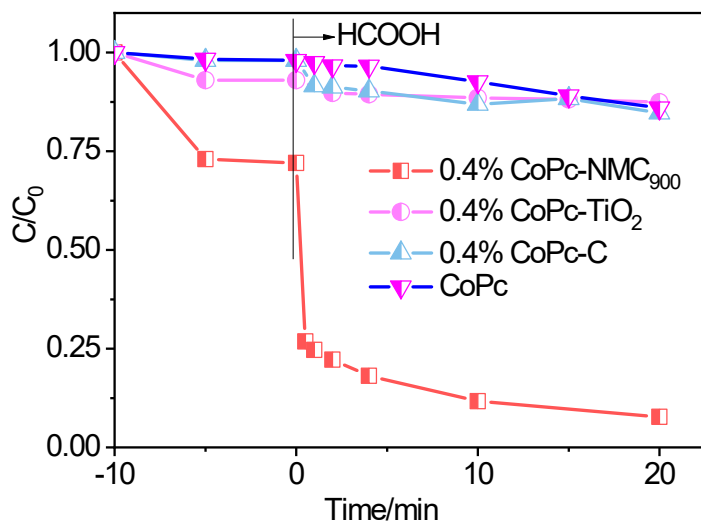
199

200 Fig. S8 (a) The influence of calcination temperature of the NMC materials on the Cr(VI)
 201 reduction. (Reaction conditions: 50 mL Cr(VI) (50 ppm), 4.3 mmol FA, 50 mg catalyst,
 202 25 °C) (b) Structure-property relationships between the normalized N species content
 203 and catalyst effectiveness for 0.4% CoPc-NMC₉₀₀.

204

205

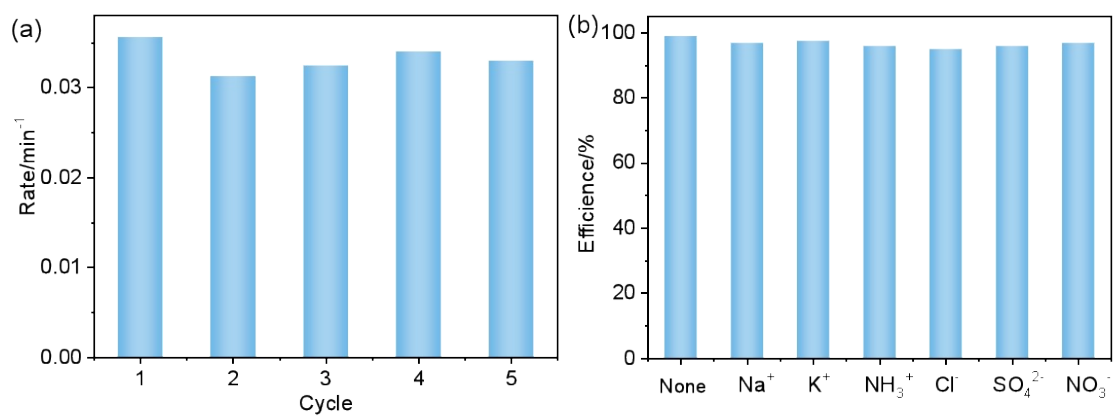
206



207

208 Fig. S9 Effect of the supports on the Cr(VI) reduction. (Reaction conditions: 50 mL
 209 Cr(VI) (50 ppm), 4.3 mmol FA, 50 mg catalyst, 25 °C)

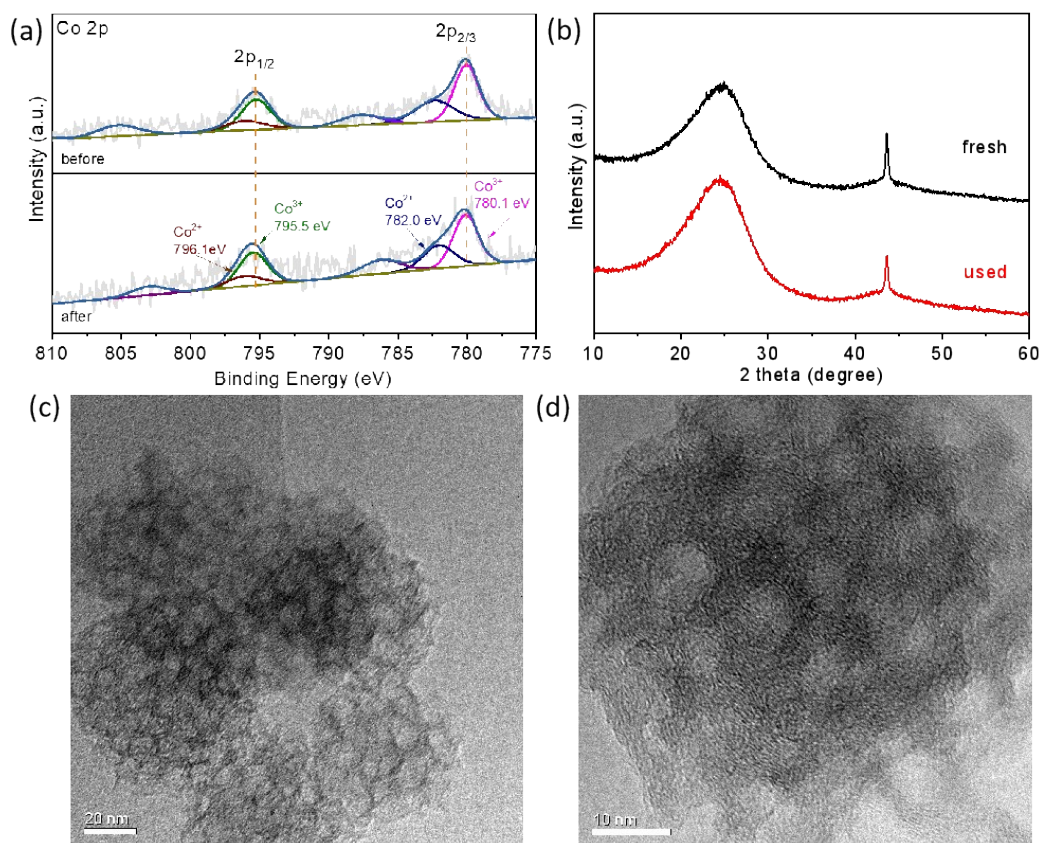
210



211

212 Fig. S10 (a) Cyclic performance of CoPc-NMC₉₀₀ for Cr(VI) reduction. (b) The
213 influence of co-existing ions. (Reaction conditions: 50 mL Cr(VI) (50 ppm), 4.3 mmol
214 FA, 50 mg catalyst, 25 °C.)

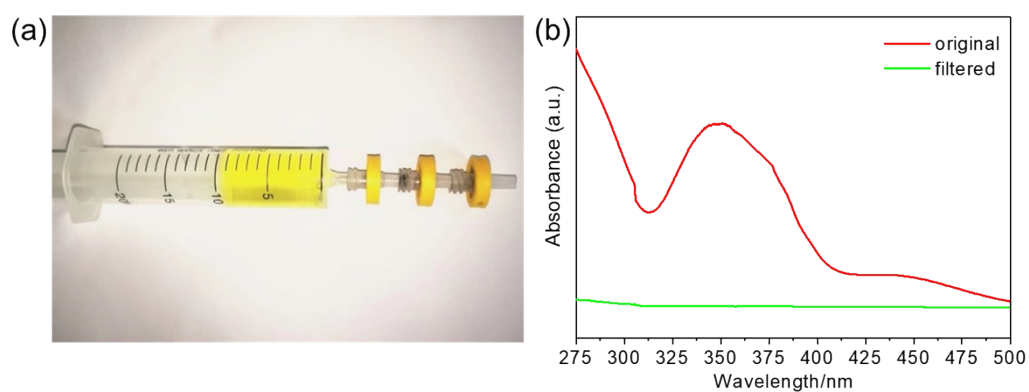
215



216

217 Fig. S11 (a) XPS of Co 2p for 0.4% CoPc-NMC₉₀₀ before and after reaction. (b) XRD
 218 pattern for 0.4% CoPc-NMC₉₀₀ before and after reaction. (c-d) TEM images of 0.4%
 219 CoPc-NMC₉₀₀ after reaction.

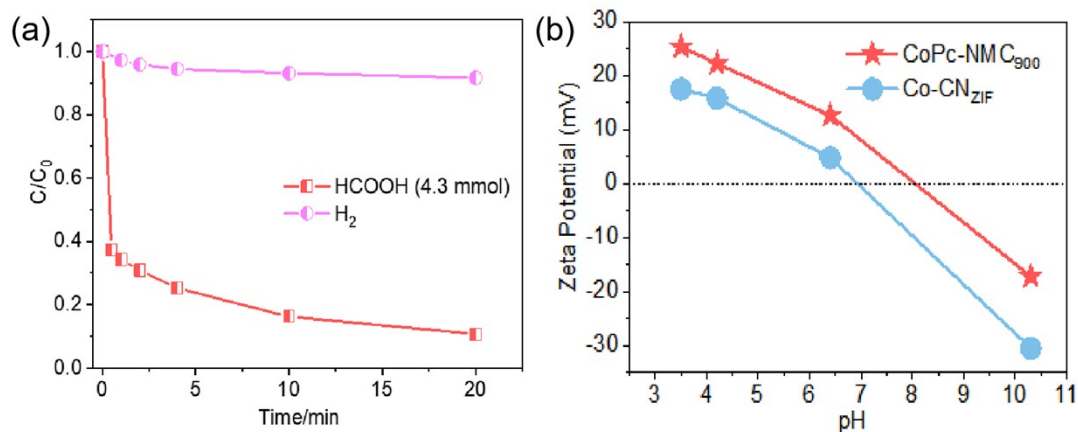
220



221

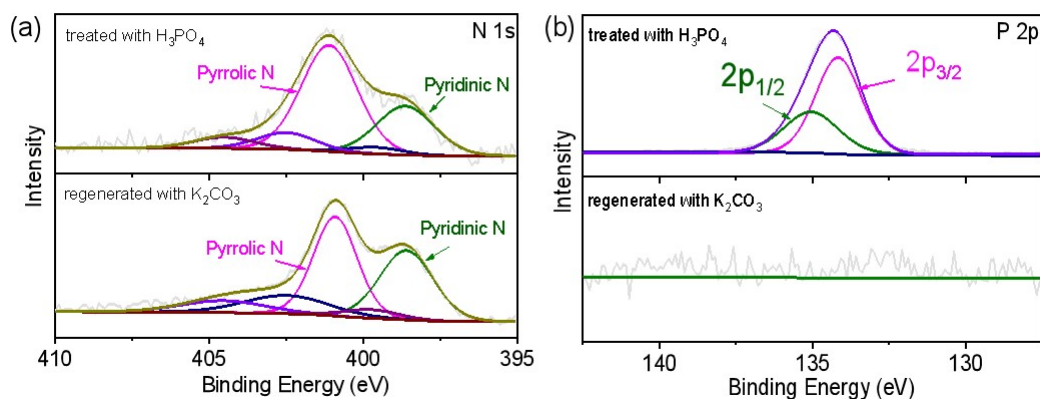
222 Fig. S12 (a) Set up of Continuous-flow for Cr(VI) reduction, (b) UV-vis absorption
223 spectra of the original and filtered solution. (Reaction conditions: 50 ppm $\text{Cr}_2\text{O}_7^{2-}$ (10
224 mL), 1 M FA, 15 mg catalyst, 25 °C)

225



226

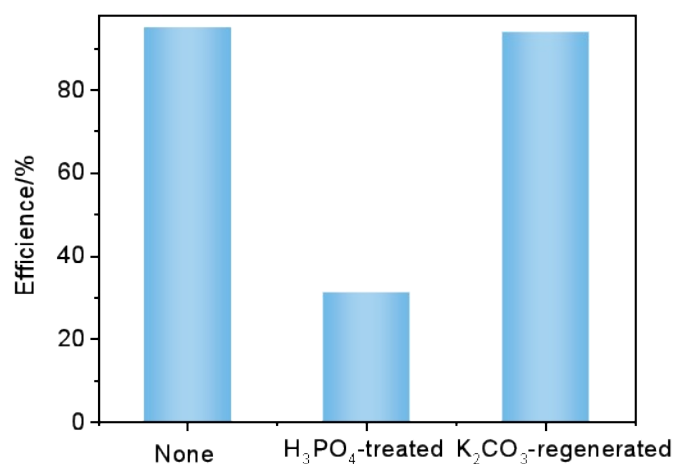
227 Fig. S13 (a) The influence of the hydrogen sources on the catalytic reduction. (Reaction
 228 conditions: 50 mL Cr(VI) (50 ppm), 50 mg catalyst, 25 °C). (b) The Zeta-potential of
 229 samples at various pH values.



230

231 Fig. S14 (a) N 1s and (b) P 2p XPS spectra for original, H_3PO_4 -treated and K_2CO_3 -
 232 regenerated samples.

233



234
 235 Fig. S15 Control reactions performed in the presence of various reagents. (Reaction
 236 conditions: 50 mL Cr(VI) (50 ppm), 4.3 mmol FA, 50 mg catalyst, 25 °C.)
 237
 238

239 Table S5 Cr(VI) reduction with D-substituted FA over the 0.4% CoPc-NMC₉₀₀.

Entry	FA	KIE
1	HCOOH	-
2	HCOOD	1.52
3	DCOOH	1.68
4	DCOOD	1.96

240 Reaction conditions: 50 ppm Cr₂O₇²⁻(50 mL), 0.1 M D-FA, 50 mg catalyst, 25 °C.

241

242

243 Table S6 Cr(VI) reduction with D-substituted FA over the 0.4% CoPc-NMC₉₀₀(H₃PO₄).

Entry	FA	KIE
1	HCOOH	-
2	HCOOD	1.05
3	DCOOH	1.09
4	DCOOD	1.12

244 Reaction conditions: 50 ppm Cr₂O₇²⁻(50 mL), 0.1 M D-FA, 50 mg catalyst, 25 °C.

245

246

247

248

249

Table S7 Cobalt-catalyzed dehydrogenation of FA^a.

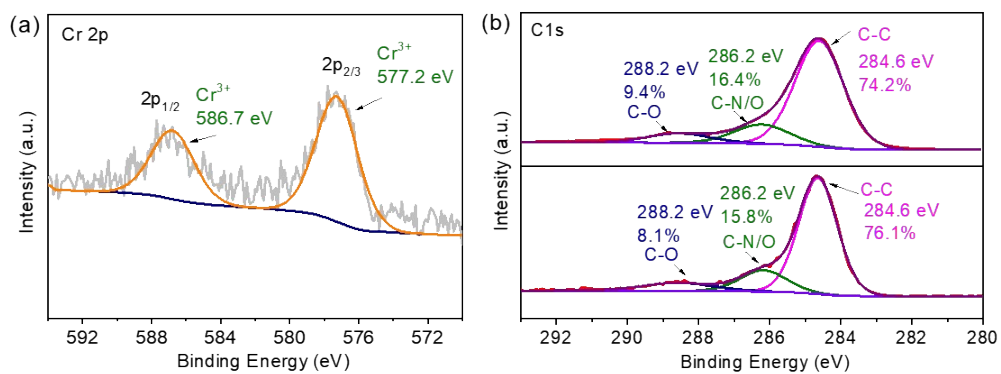
Entry	Catalysts	TOF(min ⁻¹) ^b
1	Co(NO ₃) ₂ ·6H ₂ O	0
2	NMC ₉₀₀	0
3	CoPc	6.2
4	0.4% CoPc-NMC ₉₀₀	33.5
5	CoPc-TiO ₂	7.1
6	CoPc-C	7.3
7	Co-CN _{ZIF}	106.0

250 ^a Reaction conditions: 10 mmol FA in 6 mL PC, FA/Catalyst = 1178, 110 °C. ^b Initial TOF based on
251 total amount of Co (< 15% conversion).

252

253

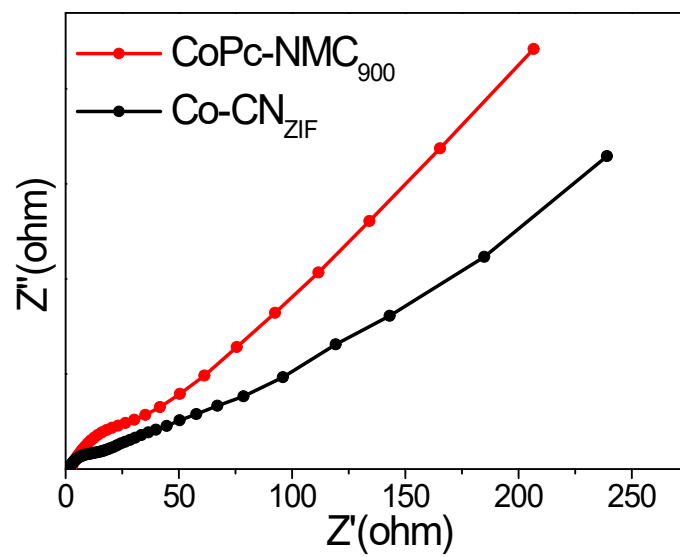
254



255

256 Fig. S16 (a) XPS of Cr 2p for 0.4% CoPc-NMC₉₀₀ after reaction, (b) XPS of C 1s for
 257 0.4% CoPc-NMC₉₀₀ before and after reaction.

258



259

260 Fig. S17 Electrochemical impedance spectroscopy of catalysts in 0.05 M KHCO_3
261 solution.

262

263 **References**

- 264 [1] Q. Zhang, M. Peng, Z. Gao, W. Guo, Z. Sun, Y. Zhao, W. Zhou, M. Wang, B. Mei,
265 X.L. Du, Z. Jiang, W. Sun, C. Liu, Y. Zhu, Y. M. Liu, H. Y. He, Z. H. Li, D. Ma,
266 Y. Cao, *J. Am. Chem. Soc.*, 2023, **145**, 4166-4176.
- 267 [2] K. Koh, M. Jeon, D. M. Chevrier, P. Zhang, C. W. Yoon, T. Asefa, *Appl. Catal. B*
268 *Environ.*, 2017, **203**, 820-828.
- 269 [3] X. Li, A. E. Surkus, J. Rabeah, M. Anwar, S. Dastagir, H. Junge, A. Bruckner, M.
270 Beller, *Angew. Chem. Int. Ed.*, 2020, **59**, 15849.
- 271 [4] C. Tang, A. E. Surkus, F. Chen, M. M. Pohl, G. Agostini, M. Schneider, H. Junge,
272 M. Beller, *Angew. Chem. Int. Ed.*, 2017, **56**, 16616.

273

274